WILEY

Thermography based breast cancer detection using self-adaptive gray level histogram equalization color enhancement method

Anthony Muthu Arul Edwin Raj[1] | Muniasamy Sundaram[2] | Thirassama Jaya[3]

[1]Electronics and Communication Engineering, Bethlehem Institute of Engineering, Karungal, India

[2]Department of Electronics and Communication Engineering, V.S.B. Engineering College, Karur, India

[3]Department of Electronics and Communication Engineering, C.S.I. Institute of Technology, Thovalai, India

Correspondence
Anthony Muthu Arul Edwin Raj, Electronics and Communication Engineering, Bethlehem Institute of Engineering, Karungal, India.
Email: aruledwinraj1021@gmail.com

Abstract

The early detection of tumor is necessary to save a number of lives. In women, the temperature of the affected area of the tumor is warmer than the unaffected area; therefore the thermography technique can be used to capture the cancerous breast images with a thermal infrared by identifying the temperature difference between them. Color enhancement of the captured breast image is an important consideration for early detection of tumor at this stage. Therefore, in this paper, we propose a self-adaptive gray level histogram equalization approach to enhance the color of the IR image for early detection of the tumor. This approach does not require any manual feeding of parameters toward images. The final classification of tumorous and non-tumorous breast images can obtain through certain procedures, which includes, image acquisition, pre-processing, segmentation, feature extraction and classification. This paper emphasizes the support vector machine (SVM) technique to classify the tumor IR thermography images. The proposed approach is implemented in MATLAB and the experimental results shows an outstanding color enhancement of IR images and better classification compared to other existing methods such as CLAHE, BIi-histogram equalization and adaptive histogram equalization. The performance was evaluated by using evaluation metrics such as sensitivity, accuracy, and specificity of thermography breast image by the SVM classifier adapted with various color enhancement approaches are found to be 91.6%, 90%, and 87.5%. This approach helps in medical field for early diagnosis with high reliability.

KEYWORDS
breast cancer, color enhancement, histogram equalization, infrared images, thermography, tumor

1 | INTRODUCTION

Nowadays the breast tumor (Cancer) rate is high among women. According to the World Health organization (WHO), 1.2 million women are affected by breast tumor and 7 lakhs women die each year.[1] Breast tumor is genetic in nature and its possibility grows with age.[2] The increase in death rate is mostly due to the lack of awareness.[3] The diagnosis of this disease can be done by the internal image of the affected area of the tumor and it is commonly done by X-ray mammography, ultrasound, MRI screening.[4] This mammography approach will

enhance the tumor growth by 2% during every examination due to electromagnetic radiations.[5] During the ultrasound screening process, the image of the tumorous region can be seen on a computer screen and can be treated by using a needle to operate normal and cancerous cells.[6] Tumor size can be detected by MRI screening procedure. Recently IR thermography-based painless detection strategy is used to detect the tumor in the breast area and it is less expensive than the above approaches.[7] This method of screening captures the images using IR cameras and works on the basis of its metabolic heat and the temperature of the tumor area based on the blood perfusion rate of the tissues.[8]

When analyzing this IR medical image for diagnosis, there may be a lack of quality due to its color and other specific conditions make it hard for the early detection of disease.[9] Nowadays, color enhancements of the IR images become a challenging task. Among all popular available techniques for color enhancement, histogram equalization plays a major role due to the simplicity and performance of images.[10,11] But at gray level equalization, the histogram approach may not perform well in managing color and brightness due to the application of the device.[12] In order to overcome this problem, some techniques like Bi-histogram equalization, multi-histogram equalization, dynamic histogram equalization and some other optimization approaches have been introduced by research scholars. It also has a drawback of remapping image peaks; time consumption and change of brightness are equal.[13] Therefore, a flat histogram approach with brightness preservation is introduced in Reference 14 but this technique will provide a low contrast image while we have a much lower or higher average brightness value. Later heuristic based optimization approaches have been considered for image color enhancement, which may work better in optimization, but it requires manual tuning of the parameters.[15]

Therefore, in this paper, we intend to propose a self-adaptive gray level histogram equalization based color enhancement in infrared thermography breast images for early detection of tumor. Here the color brightness of the image is achieved through power law transformation approach. The features are extracted using discrete wavelet transform (DWT), gray level co-occurrence matrix (GLCM), and principle component analysis (PCA).

DWT is a linear transformation where mammography image information is divided into detailed and approximation parts. These parts can be achieved by implementing the high pass and low pass filters on mammogram respectively. PCA is used for feature space dimensionality reduction, that is, principal components (PCs) are sufficient to classify the mammograms.[16] DWT provides better brightness of the image, GLCM provides information about GLCM pixels and PCA approach will reduce the dimension and complexity in extracting the features. Finally, for classifying the tumorous and non-tumorous images SVM[17,18]classifier is used. The rest of the paper is summarized as follows: Section 2 provides various recent research works on contrast enhancement and tumor detection. Section 3 provides a detailed study of our proposed methodology and Section 4 delineates the implementation and analysis of the suggested approach and finally Section 5 concludes the paper with its future direction.

2 | LITERATURE REVIEW

Various investigation works have earlier existed at bibliography that relied on color or contrast enhancement of IR thermogram images and early detection of cancer tumor has been presented. Table 1 delineates the brief description on concerned papers under literature survey.

Marin et al.[19] presented a device based on contact thermography related to the detection and localization of breast cancer in the early stages of disease. To achieve a difference and normalized fields on the breast surface they used two temperature sensor arrays, a junction diode array and NTC sensor array so that they could identify the presence of tumor based on distractions. In addition, they used a penne's equation to solve the inverse temperature field problem when the tumor was detected. Finally, the obtained data has been seen clearly through a specially designed GUI which showed the uniqueness of their research work.

Roy et al.[20] proposed a breast cancer detection approach by combining the mammography and thermography based on the fractal features of abnormal regions of the breast. Their combined fractal approach analyzed using the mini-MIAS mammogram dataset has achieved the prediction accuracy of about 95.94% and seemed to be the most efficient with texture features 79.31% and 78.94% detected the affected breast region.

Singh et al.,[21] presented a review of image acquisition protocols, segmentation techniques, feature extraction and classification methods were used in breast thermography at recent years. The comprehensive survey emphasized the improved accuracy of the breast thermograph. The use of machine learning techniques to properly classify breast thermogram was studied. In thermographic diagnosis, the numerical simulation can be used as a support tool to resolve high false positive levels.

Dhal et al.[22] have proposed a nature-inspired optimizing algorithms (NIOAs) used for multi-threshold problem. Multi-thresholding was one of the most important image segmentation techniques in image processing.

TABLE 1 Literature review

Year	Author	Title	Proposed methodology	Outcome
2018	Marin, M. E.	Testing of two thermographic devices with two types of temperature sensors for detecting and locating of incipient breast tumors	The BAV99 has two series junction diodes in a SOT23 package as a first temperature sensor and NCP18XH103F03 10 kΩ NTC as the second sensor	Detection and localization of early breast cancers
2017	Roy, Anindita	Early breast abnormality based on fractal feature prediction	Designing of the DBT-TU-JU breast thermogram database using fractal features	Efficiency of dimension and lacunarity fractal features: on breast mammograms and thermograms on breast has been delineated.
2019	Singh, Deepika, and Ashutosh Kumar Singh	Role of image thermography in early breast cancer detection—Past, present, and future	Thermographic techniques based on accuracy, advances in machine learning techniques and the study for practical relevance has been reviewed.	The study presents various segmentation, feature extraction and classification techniques used in breast thermography.
2019	Raghavendra, U.	Computer-aided diagnosis for the identification of breast cancer using thermogram images: A comprehensive review	Explored machine learning based approaches	Implementation of a deep neural convolution network for breast thermograms will improve overall reliability and might be a hard-term solution for aggressive early detection of breast cancer
2018	Díaz-Cortés, Margarita-Arimatea	A multi-level thresholding method for breast thermograms analysis using dragonfly algorithm	Multi-thresholding task is performed using dragonfly algorithm (DA)	DA-breast thermography thresholding (DA-BTT) outperforms facilitate the labor of heath-professionals in diagnosis and monitoring of breast cancer in cheap and it is more accessible to transport
2018	Gonzalez-Hernandez, Jose-Luis et al.	Technology, application, and potential of dynamic breast thermography for the detection of breast cancer	Dynamic infrared thermography approach	Improve the detection of breast cancer and reduce the false positive and false negative rates
2017	Tan, Siu Fong, and Nor Ashidi Mat Isa	Exposure based multi-histogram equalization contrast enhancement for non-uniform illumination images	Modified HE-based contrast enhancement technique	More uniform illuminate image with better contrast, highest PSNR, lowest AMBE as been achieved.
2017	Kallel, Fathi, and Ahmed Ben Hamida	A new adaptive gamma correction-based algorithm using DWT-SVD for non-contrast CT image enhancement	Adaptive gamma correction algorithm	Enhanced the non-contrast CT images and achieved the overall quality and visibility
2019	Vijaya Madhavi and Christy Bobby Thomas	Multi-view breast thermogram analysis by using texture features	Analysis the performance of detecting breast cancer by combining multiple visions of thermograms.	The LSSVM classifier enables an optimal hyper-parameters to classify normal and abnormal subjects
2019	Devi, R. Ramya, and G. S. Anandhamala	Analysis of breast thermograms using asymmetry in infra-mammary curves	A method of analyzing breast thermograms to detect breast abnormalities, including cancer.	The heat patterns are analyzed by symmetry and asymmetric analysis helps to detect abnormalities.

TABLE 1 (Continued)

Year	Author	Title	Proposed methodology	Outcome
2019	Abdel-Nasser, Mohamed, Antonio Moreno, and Domenec Puig	Breast cancer detection in thermal infrared images using representation learning and texture analysis methods	Using a representative learning technique and system analysis methods for breast cancer detection.	Generates a compact representation for the infrared images, which exploits the differentiations between normal and cancerous cases.
2019	Jeyanathan, Josephine Selle, et al.	Jeyanathan, Josephine Selle, et al. Analysis of transform-based features on lateral view breast thermograms	The efficiency of breast thermograms in lateral views is statistically analyzed.	Attempted methods of lateral vision analysis, the accuracy rate due to the AdaBoost algorithm is increased in the lateral view.

Thresholding is considered as a pixel classification problem. There were two types of thresholding models such as bi-level and multi-thresholding. Nature-inspired optimization algorithms (NIOAs) were used to solve complex optimization problems.[22,23]

Chakraborty et al.[24] have proposed a computer-aided detection (CAD) method for automatic detection of masses in mammograms.[25] This approach used a multi-level threshold method to regional growth and false positives in 3D imaging, and also presented the process of detection and segmentation in image processing, where the threshold followed an iterative model to reduce the intensity of mass region development and the intensity of mass region gradually decreases.[26]

Raghavendra et al.[27] analyzed a computer-aided diagnostic system based on thermogram developed for the detection and breast cancer examination. They discussed the quantitative and qualitative quality of machine-based learning approaches, including segmentation-based methods and extraction-based functionality, dimensionality reduction, and various classification schemes proposed by various researchers. They also suggested future directions for further improvement in current approaches.

Diaz-Cortes et al.[27] proposed a thermographic image segmentation technique that took into account of pixel spatial information of the image. This method used a new technique of optimization called the dragonfly algorithm to calculate the best thresholds for image segmentation. The results of the experiment showed the good performance of the proposal in many ways relative to other methods. This approach helped in the medical field for early diagnosis with high reliability.

Gonzalez-Hernandez et al.[28] introduced a dynamic infrared thermography strategy to improve the identification of breast cancer and increasing false positive and false negative rates. The research examined the various methodologies of dynamic infrared thermography, their strengths, limitations and future growth opportunities. This paper also deals with the recent progress, recommendations and potential directions for the future field of dynamic infrared thermography to improve the detection efficiency.

Tan et al.[29] proposed an advanced adaptive and simple algorithm for improving the dark medical image. Performance was evaluated primarily on the basis of adaptive gamma correction using discrete wavelet transformation with decomposition of singular value (DWTSVD), the performance evaluation had been done. They proposed a contrast enhancement algorithm. It was based on adaptive gamma correction utilizing discrete wavelet transform with singular-value decomposition. The performance of the algorithm had been evaluated on different types of non-contrast CT clinical image.

Madhavi et al.[30] have analyzed the effectiveness of detecting breast cancer in the screening phase by combining significant system features derived from multiple vision thermogram. Regional structure features are extracted for 32-normal and 31-abnormal features are selected from DMR database. Using the *t*-test, the reduced feature set is determined from the front, right-lateral and left-lateral thermogram independently for extracting the system features. The experimental results show that 96% classification accuracy, 100% sensitivity, and 92% specification are achieved using the LSSVM classifier that uses optimal hyper-parameters.

Devi et al.[31] introduced a method of analyzing a breast thermogram to detect breast abnormalities, including cancer. This research work is mainly aimed at the separated ROI, which shows a significant increase in temperature compared to the interactions with neighboring regions and breast thermogram. They have analyzed the heat patterns of the symmetry and the asymmetry analysis helps to detect abnormalities.

Abdel-Nasser et al.[32] proposed a new method to model temperature changes in normal and abnormal breasts using a representative learning technique known as learning-to-rank and system analysis methods. This method generates a compacter presentation of the infrared images of each sequence, which is then exploited to differentiate between normal and cancerous cases. The experimental result shows that the proposed method achieved a high accuracy of 98.9% compared to other methods.

Jeyanathan et al.[33] analyzed the efficiency of breast thermogram in lateral views. In order to classify the normal and abnormal breast thermogram, the features were analyzed by using an independent *t* test to decide if lateral view breast thermogram has any effect on the classification accuracy. The overall classification result shows the lateral view thermogram to exhibit higher accuracy rate as compared to the front view. In lateral vision analysis, the accuracy rate due to the Ada Boost algorithm was increased to 91% in lateral view, which was reduced to 83% in front view.

3 | PROPOSED METHODOLOGY

Breast cancer (tumor) is one of the deadliest diseases found among women nowadays; it can be cured majorly at the early stage of disease. Here in this paper, we put an effort to enhance the contrast (color) of the thermography image to support the disease diagonalization at the early stage. Initially the captured IR images have been enhanced by using the self-adaptive gray level histogram equalization approach. This approach will efficiently enhance the color of the image and provides the quality images for further feature extraction by DWT and GLCM. Finally, the SVM classifier is used to classify normal and abnormal thermography breast images. This suggested approach will provide better guidance for breast cancer detection based on observable and qualitative tests measured from the thermography IR images of the breast.

3.1 | Breast thermography

Breast thermography is the process of measuring the inner breast surface temperature by means of an infrared camera in order to differentiate the tumorous and non-tumorous region. In addition, by knowing the blood perfusion and metabolic activity in tumorous and non-tumorous region, we can able to identify the fastest growing and slow growing tumors. This approach is trending for early detection of tumor due to its advantages like less cost, contactless, non-invasive, painless when compared to mammography screening approach.

Figure 1 shows the tumorous and non-tumorous women breast images,[21] the tumor can be found in any part of the breast. This breast thermography is a radiation free process and inexpensive. During this process, for about 15 minutes the patient will be endured in a room temperature of about $18°C–25°C$. The temperature level of the tumorous region will be higher than the normal region, therefore the IR signal is transferred and the heat map of the breast is given to us and the surrounding tissues are digitalized and saved in the system, which helps in early detection of the disease. A diagnostic screening technique's sensitivity is a measure of the rate at which a tumor is detected. The higher sensitivity, the higher chance of a tumor will be found in a person. According to planks[34] the temperature of the breast emits can be calculated based on IR radiation intensity, which is given in Equation (1).

$$I(\omega, T) = \frac{2\pi h c^2}{\sigma^2} \left(e^{\frac{hc}{ikT}} - 1 \right) - 1 \tag{1}$$

where I is the intensity of radiation, ω is the wavelength, T is the temperature, h is the Planck constant, c is the speed of light in vacuum, and k is the Boltzmann constant.

The emitted IR radiation can be evaluated by using the Stefan Boltzman equation in (2),

$$E = \in \sigma T^4 \tag{2}$$

where E is the total emissive power (W/m^2), σ is the Stefan Boltzmann's constant (5.676×10^{-8}), T is the absolute temperature.
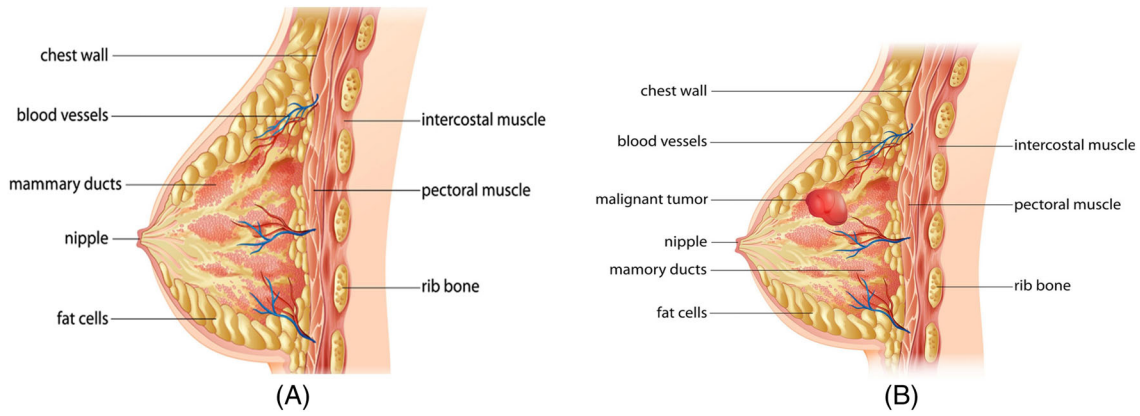
FIGURE 1 Breast anatomy. A, Normal; B, tumorous [Color figure can be viewed at wileyonlinelibrary.com]

The skin emission is 0.989 ± 0.01 self-reliantly to its color; lower the sensitivity greater detection of temperature variation while capturing the thermal images. Here, in order to obtain a quality thermography image for better and sooner diagnostician of disease color enhancement is necessary. In thermogram image red, orange, and yellow colors represents the warmer region of breast, that is, presence of tumor and purple, dark blue or black represents the normal region.[35] Therefore, the color enhancement of the thermography images plays a crucial role while diagnosing and upcoming section describes the following enhancement algorithm in detail.

3.2 | Preliminaries

3.2.1 | Histogram equalization

It is an elegant and efficient approach in image color enhancement and it is mainly analyzed in terms of probability, cumulative and transfer function. The IR image captured by the camera is represented as,

$$Y = Y(i,j) \tag{3}$$

The gray level discrete component of the image is represented as,

$$L = \{Y_0, Y_1, \ldots\ldots Y_L\} \tag{4}$$

The PDF (probability distributive function) is represented as in equation.

$$P(Y_k) = \frac{n^k}{n} \text{ for } k = 0, 1, \ldots\ldots, L-1 \tag{5}$$

where n^k is the occurrence of the gray level k in the image, and L is the total number of gray levels in the image and n is the total number of pixels in the images.

The CDF (cumulative distributive function) is represented as in equation,

$$C(Y_k) = \sum_{n=0}^{k} P(Y_k) \tag{6}$$

The TF (transfer function) is represented as $F(Y)$ and it is based on the cumulative distributive function of the system[36] and the final color enhanced image is represented as,

$$X = f(Y) \tag{7}$$

3.2.2 | Bi-histogram equalization

The captured IR image is subdivided into two sections by separating the mean gray level as Y_L and Y_u in each subdivided section is termed as Bi-histogram equalization, which is represented as in equation.

$$Y = Y_L \cup Y_U \text{ and } Y_m \in \{Y_0 + Y_1 + \ldots + Y_{L-1}\} \tag{8}$$

where Y_m is the mean value

The PDF of this subdivided images can be represented as,

$$P_L(Y_K) = \frac{n^k L}{n_L} \quad \text{where} \quad K = 0, 1 \ldots, m \tag{9}$$

$$P_U(Y_K) = \frac{n^k U}{n_U} \quad \text{where} \quad k = m+1, m+2, \ldots\ldots, L-1 \tag{10}$$

where n_L and n_U are the total number of pixels in the lower and upper histograms, respectively.

The CDF of the subdivided image can be represented as,

$$C_L(y) = \sum_{n=0}^{k} P_L(Y_j) \qquad (11)$$

$$C_U(y) = \sum_{n=0}^{k} P_U(Y_j) \qquad (12)$$

In Bi-histogram equalization also, TF is based on CDF[37] and the final color enhanced image can be represented as,

$$X = X(i,j) \qquad (13)$$

where (i, j) are the spatial coordinates of the pixel in the image.

3.2.3 | Adaptive histogram equalization (AHE)

This is an image processing approach, which plays a crucial role in image contrast enhancement by the number of histograms instead of single ordinary histogram equalization. Here, the histogram is evaluated from a distinct section of the image to reschedule the lightness values of the image to full scale. This AHE bring out the image darkest portion details for more improvement while enhancing the image contrast, since there is a problem of significant production of noise.

When intensity level x (i, j) of the center pixel of window W has no image detail, the condition for the adaptive adjustment process of k: $k \rightarrow 0$; otherwise, $k \rightarrow$ larger value. K can be expressed as the intensity level variance of the window W neighborhood, which is described as.

$$k = k'\left(\left(\sigma^2(i,j)\right)/\left(\sigma^2 n\right) - 1\right) \qquad (14)$$

where $\sigma^2(i, j)$, $\sigma^2 n$ is the intensity level, variance of window W and the noise variance of whole image intensity level, respectively. k' is the proportional.[38]

3.2.4 | Contrast limited adaptive histogram equalization (CLAHE)

The noise over amplification problem by the AHE can be disabled by clipping before the cumulative distributive function evaluation is termed as contrast limited adaptive histogram equalization (CLAHE). Here, the original $M \times N$ input image is divided into many non-overlapping contextual regions. The flowchart for CLAHE is given in Figure 2.

In order to enhance the color of the image, the intensity value of the image have to be enhanced here by means of Raleigh transform[39] which is represented as in Equation (15),
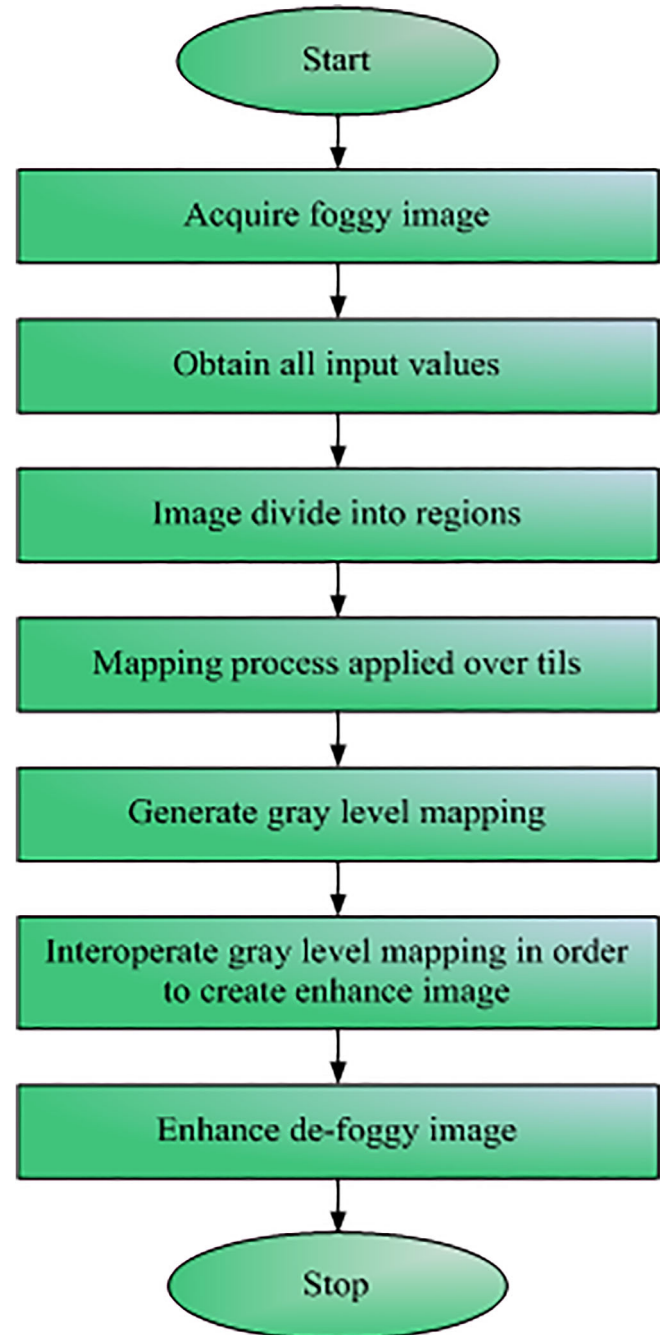
FIGURE 2 Flow chart for CLAHE [Color figure can be viewed at wileyonlinelibrary.com]

$$Z(i) = Z_{\min} + \sqrt{2\beta^2 \ln\left(\frac{1}{1 - P_{input^{(i)}}}\right)} \qquad (15)$$

where Z_{min} is the lower bound of the pixel value and β is the scaling parameter of Rayleigh distribution.

3.2.5 | Asymmetry analysis

The features derived from the testing images, the existence of asymmetry is decided by calculating the ratio of the feature from left and right segment. The closer value to 1, the more correlated features or the less asymmetric segments.

3.2.6 | Modified histogram equalization

Consider that the thermography image captured by the IR camera be $I = \{I(I,j)|1 \le i \le M, 1 \le j \le N$ with the size of about $M \times N$ pixels, in which the $I(i, j) \in R$ (0-255). The IR image probability density function of normal histogram equalization (HE) (Figure 3) can be evaluated by using Equation (16),

$$P(K) = \frac{nk}{j} \text{ for } k = 0, 1, 2, \dots, L-1 \qquad (16)$$

where nk is the pixel number with intensity k and J,

$$c(k) = \sum_{i=0}^{k} p(i) \qquad (17)$$

where $c(k)$ is the cumulative distribution function.

The gray level will be in 0, 1,..., $L - 1$ interval in which the value of L is 255 for an image with 8 bits, the transformation mapping $T(k)$ for normal histogram equalization can be obtained by multiplying $c(k)$. The

FIGURE 3 Histogram equalization [Color figure can be viewed at wileyonlinelibrary.com]

transformation function $T(k)$ can be evaluated by using Equation (18),

$$T(k) = [(L-1)c(k) + 0.5]; 2^b = L \qquad (18)$$

where b is the bit image, the probability occurrence of kth gray level of image is directly proportional to transformation function, which is represented as in Equation (19),

$$\Delta T(k) = T(K) - T(K-1) \cong (L-1)p(k) \qquad (19)$$

The spikes and noise from the original histogram can be removed by using the following modified histogram equalization is given in Equation (20),

$$h_{mod}(i) = p[i(c)] \qquad (20)$$

where $p[i|C]$ is the probability occurrence of ith gray-level, C is the horizontal contrast variation.

A default value of sis will be assigned to CAS and it fits well for all image types. The h_{mod} value must be normalized to keep the value in between 0 and 1 based on the pixels under consideration. The unique parameter to weigh the h_{mod} can be evaluated by using Equation (21),

$$h = wh_i + (1-w)u \qquad (21)$$

where w is the weighing factor (0-1).

The uniform probability density function (u) can be evaluated by using Equation (22),

$$u = ones\frac{L,1}{L} \qquad (22)$$

The clipped histogram can be attained from h_i can be evaluated by using the equation,

$$h_{modc}(k) = \begin{cases} \frac{1}{L} if h_i(k) > \left(\frac{1}{L}\right) \\ h_i(k) if h_i(k) \le \left(\frac{1}{L}\right) \end{cases} \qquad (23)$$

The measure of un-equalization can be evaluated by using Equation (24),

$$M_u = sum(u - h_{modc}) \qquad (24)$$

The value obtained from Equation (24) represents the degree of images which omit to follow the uniform distribution. The probability distribution function of the
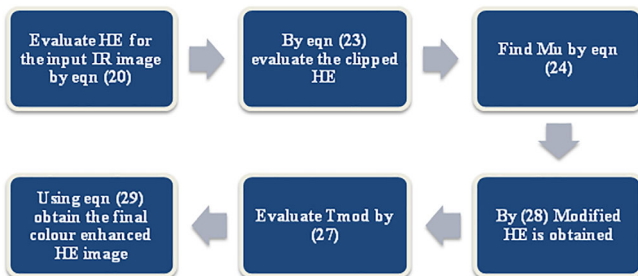
modified histogram equalization can be evaluated by using Equation (25).

$$h_E = (Mu)h_{mod} + (1 - Mu)u \qquad (25)$$

The cumulative distributive function of the modified histogram equalization can be evaluated by using Equation (26),

$$C_E(k) = \sum_{i=0}^{k} h_{SAGHE}(k) \qquad (26)$$

The transformation function of the proposed equalization[40] is given as in Equation (27),

$$T_{mod}(k) = [(L-1)C_{SAGHE}(k) + 0.5] \qquad (27)$$

The output image of hmod can be represented as in Equation (28),

$$I_E = \{I_{SAGHE}(i,j)\} = \{T(I(i,j)) \forall I(i,j) \in I\} \qquad (28)$$

3.2.7 | Self-adaptive gray level histogram equalization based on power law transformation

The color of the histogram equalized modified image can be enhanced by means of a power law transformation, which is of the form,

$$s = r^{\gamma} 0 < \gamma < 1 \qquad (29)$$

The average intensity of the self-adaptive factor after the HE can be evaluated by using Equation (30),

$$\gamma = \frac{\log(mean(I_{SAGHE}))}{\log(255)} \qquad (30)$$

The value of γ obtained by the above equation varies from 0 to 1, for brighter image gets closer to "1" and for darker images, "0." Relative to dark image, this adaptive correction is necessary for the bright color image.

Power law transformation is an image enhancement technique which usually creates a better-looking image by adjusting the intensity depending on gamma value. The method adopted for the generation of multiple exposure images is by varying the gamma value. The basic equation of power law transformation is given by,

$$R = D^{\gamma} \qquad (31)$$

where R is the output image, D is the input image, and γ is the gamma value. Changing the gamma value generates different images have different exposures. Input image is first converted into its HSV color space because RGB color information is often more noisy than HSV information. Power law transformation is applied to the V-channel of the input image for generating the multiple exposure images. The ideal value of gamma is assumed to be one. But the variation in gamma value beyond a particular limit completely degrades the image. So in order to prevent the degradation, the value of gamma should be limited within a particular range. The gamma value range is selected so that the entropy of multiple exposure images is not less than a particular threshold value.

We propose a self-adaptive gray level histogram equalization based on color enhancement without altering the hue of any image pixels, because HUE is the crucial component in maintaining the color of the thermography IR image. By using Equation (20) the input images are evaluated. The Histogram clipped images are evaluated using Equation (23). Then measure the un-equalization values. The changes in HUE affects the quality of the captured IR image, therefore the saturation and HSV image value is processed and power law transformation is applied to the hue component if needed with the marginal γ value. Then HE is modified by applying Equation (28) and T mod is evaluated. Finally get the color HE image. This approach will simplify the past gray scale image enhancement to color image and the gamut problem can be overwhelmed by removing the power law transformation ($\gamma = 0$) if necessary.

The probability of occurrence of gray level r_a in an image V is,

$$P_V(r_a) = \frac{n_a}{n} a = 0, 1, 2, 3, ..., L-1 \qquad (32)$$

where n is the total number of pixels in the image, n_a is the number of pixels that have gray level r_a, L is the total number of possible gray levels in the image, $P_V((r_a)$ vs r_a is called a histogram.

The cumulative distribution function corresponding to $P_V(r_a)$ is represented as in equation,[33]

$$S_V = T(r_a) = \sum_{j=0}^{a} P_V(r_j) a = 0, 1, 2, ..., L-1 \qquad (33)$$

Consider the gray scale image of the input RGB image is Y (reference image). Its probability distributed function is represented as in Equation (34),

$$P_Y(r_b) = \frac{n_b}{n} b = 0, 1, 2, 3, ..., L-1 \qquad (34)$$

The cumulative distribution function corresponding to $P_Y(r_b)$ is represented as in Equation (35),

$$S_Y = T(r_b) = \sum_{i=0}^{b} P_Y(r_i) \quad b = 0, 1, 2, ..., L-1 \tag{35}$$

Each gray level (r_a) in V is equalized to gray level (r_b) in Y is represented as in Equation (36).

$$P_{v(r_a)} = P_{y(r_b)} \quad orr = G^{-1}(P_v(r_i)) \tag{36}$$

Produce a new image $\{y\}$, from $y = T(x)$ transform, by Equation (27).

Pseudo code for SAGHE

Initially, the unnecessary portion of the IR image is cropped and resized to a suitable size based on the application

Converted RGB image to HSV image

Convert input RGB image to gray consider as a reference image

Apply power law to the hue component if necessary

Avoid the power-law by doing $\gamma = 0$

(Few images require power-law transformation with marginal γ value)

if

Histogram equalization for S component

else

Probability and cumulative distributive function of the value component of HSV image is evaluated

Formation of new image with flat histogram

Recombine HSV components

Finally, convert HSV to RGB for enhanced image

End

3.3 | Early detection of tumor in infrared thermography breast images

Thermography is a technique of determining the average temperature area of a body which includes the need for an IR camera. An anomaly in breast surface temperature may indicate a tumor's presence. Cancer cells have significantly higher metabolism in the early stages than healthy cells. This, along with the actuality that the blood vessels of the tumor are not yet developed, gives it high power density and it produces more pressure on the surface of the skin. Thermography has certain series of specific criteria must be followed to achieve accurate results using IR thermography are described as follows.

3.3.1 | Image acquisition

The patient under the diagnostic process is asked to wait in a temperature-controlled room for about 15 minutes, so that, they will get relaxed and there is no tiredness and metabolism rate is stable. The IR camera mounted on the tripod with a laser pointing to the breast[41] of the patient is fixed appropriately. Based on the temperature variation of the inner breast area, the camera will capture the thermography breast image of the patient. For performance evaluation, the available FLIR dataset[42] of thermal image has been used. A total of 40 thermography images of the breast including 24 normal and 16 malignant is analyzed.

3.3.2 | Pre-processing

The IR image captured will be different size and in order to locate tumorous region, the particular area should be cropped to a pixel value based on the requirement and the presence of noise while capturing the image will be removed in this pre-processing.[40] This gray scale pre-processed thermography breast image will further use for segmentation and feature extraction process.

3.3.3 | Segmentation

In this stage based on the Region of interest (ROI), the left and right breast thermography image is segmented. In this stage based on the Region of interest (ROI) segmentation; the ROI was segmented from the input images. The segmented ROI is enhanced using various methods such as CLAHE, Bi-histogram equalization, adaptive histogram, histogram equalization and proposed methods for normal and malignant images separately. Using the ROI-based segmentation; the left and right breast thermography image will be segmented. In thermogram image red, orange and yellow colors represent the warmest region of the breast that is the presence of tumor: and purple, dark blue or black represents the normal region. Therefore, the color enhancement of the thermography images plays a crucial role in the image segmentation.

3.3.4 | Feature extraction

In this stage, the spatial domain features such as contrast, correlation, energy, homogeneity, mean, SD, entropy, RMS, variance, smoothness, kurtosis, skewness, and IDM were extracted based on the probability of finding a gray-level pair at random distance and orientations over the whole image, which is also known as gray-level co-occurrence matrix (GLCM).

3.3.5 | Classification

Support vector machine (SVM) is a classification machine learning algorithm given an input infrared image, the major task of this SVM classifier is to decide whether an image is normal or malignant.

Figure 4 shows the clear image of the proposed thermography breast image color enhancement approach, Here, the region of interest (ROI) was segmented from the input image; the segmented ROI is enhanced using various enhanced methods such as CLAHE, Bi-histogram equalization, adaptive histogram, histogram equalization and proposed methods for both normal and malignant images separately. About 13 statistical features were extracted using four levels of discrete wavelet transform (DWT). From the analysis, it is noticed that about seven features have considerable variation between normal and malignant images. The principle component analysis (PCA) applied to the shortlisted seven features. Finally, the classification task decides whether an image is normal or malignant. The statistical features, before input into the SVM, might have gone through principle component analysis (PCA). PCA is normally used when the feature set is very large or contains redundant features.[41,28] Support vector machine (SVM) classifier was trained using these shortlisted features, after enhancement it is easy to fix the hyper-plane for classification.

4 | IMPLEMENTATION ANALYSIS

The evaluation of the proposed thermography breast image color enhancement approach is implemented in MATLAB and its performance is compared with the existing CLAHE, Bi-histogram equalization and adaptive histogram equalization. The thermogram of the person with cancer tumor is considered as the abnormal thermogram and without tumor is considered as the normal thermogram.

4.1 | Evaluation metrics

The performance is assessed by the metrics such as Sensitivity, Accuracy, Specificity, FPR and TPR and it is defined as in Equations (37)–(41).

4.1.1 | Sensitivity

Measures the proportion of positive cases which are correctly identified as positive,

$$\text{Sensitivity} = \frac{TP}{TP + FN} \tag{37}$$

4.1.2 | Accuracy

Percentage of correct classification,

$$\text{Accuracy} = \frac{TP + TN}{TP + TN + FP + FN} \tag{38}$$

4.1.3 | Specificity

Measures the proportion of negative cases which are correctly identified as negative,

$$\text{Specificity} = \frac{TN}{TN + FP} \tag{39}$$

The false positive rate is also called miss rate, which can be calculated by,

$$\text{FPR} = \frac{FP}{FP + TN} \tag{40}$$

FIGURE 4 Proposed thermography breast image color enhancement and classification [Color figure can be viewed at wileyonlinelibrary.com]
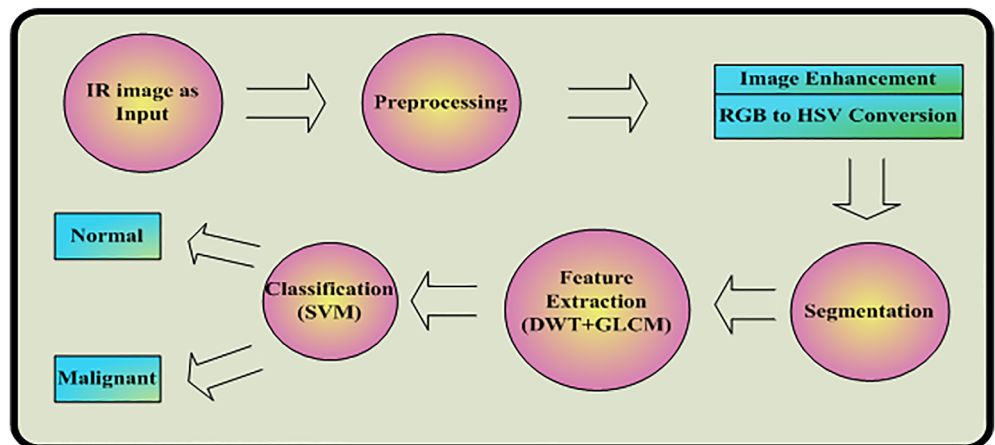
4.1.4 | True positive rate (TPR)

The true positive rate is also called as sensitivity, which is calculated as,

$$TPR = \frac{TP}{TP + FN} \tag{41}$$

where *TP* is true positive (malignant image), *TN* is true negative (normal image), *FP* is false positive (normal cases identified as abnormal) and *FN* is false negative (abnormal cases identified as normal).

4.1.5 | Area under the curve (AUC)

It measures the quality of the model's predictions irrespective of classification threshold is chosen. In our proposed method area under the curve value = 0.981 (Figure 5).

4.2 | GLCM features

Gray-level co-occurrence matrix (GLCM) features such as contrast, correlation, energy, homogeneity, mean, SD, Entropy, RMS, variance, smoothness, kurtosis, skewness, and IDM; they were extracted based on the probability of finding a gray-level pair at a random distance and orientations over the whole image.

4.2.1 | Mean

Mean is defined as the first statistical features and the average color of the image. It can be determined by the following formula,

FIGURE 5 AUC value of our proposed system [Color figure can be viewed at wileyonlinelibrary.com]

$$Mean = \sum_{i=0}^{k-1} i.p(i) \tag{42}$$

4.2.2 | Variance

Variance is a measure of the dispersion of the values around the mean.

$$Variance = \sum_{i=0}^{k-1} (i-\mu)^2.p(i) \tag{43}$$

4.2.3 | SD

The SD is estimated by taking the square root of the variance in mean value.

$$SD = \sqrt{\sum_{i=0}^{k-1} (i-\mu)^2.P(i)} \tag{44}$$

4.2.4 | Skewness

Skewness helps to measure the degree of histogram asymmetry around the mean.

$$Skewness = \sigma^{-3}\left[\sum_{i=0}^{k-1} (i-\mu)^3.P(i)\right] \tag{45}$$

4.2.5 | Kurtosis

Kurtosis formula represents a measure of the sharpness of histogram.

$$Kurtosis = \sigma^{-4}\left[\sum_{i=0}^{k-1} (i-\mu)^4.P(i)\right] \tag{46}$$

4.2.6 | Entropy

Entropy shows the amount of image information that is needed for image compression. Entropy measures the

information loss and also measures the image information.

$$Entropy = -\left[\sum_{i=0}^{k-1} P(i).log_2[P(i)]\right] \quad (47)$$

4.2.7 | Contrast

It is the measure of local intensity variation and how the gray levels vary with the image and to extent their distribution is biased to black or white.

$$Contrast = \sum_{p=0}^{L-1} P^2 \left\{ \sum_{i=1}^{K}\sum_{j=1}^{K} p(m,n) \right\}, |m,n| = p \quad (48)$$

where $p(i, j)$ is the intensity value of the pixel at the point (i, j) and m, n is the size of the image.

4.2.8 | Energy

Energy is a measure of local homogeneity and therefore it represents the opposite of the entropy.

$$Energy = \sum_{i=0}^{K-1}\sum_{j=0}^{K-1} \{P(i,j)\}^2 \quad (49)$$

4.2.9 | Dissimilarity

The dissimilarity measure is robustly related to high spatial frequencies in the texture of a breast ROI image.

$$Dissimilarity = \sum_{i=0}^{K-1}\sum_{j=0}^{K-1} |i-j|.P(i,j) \quad (50)$$

4.2.10 | Correlation

It is the measure of the relationship among the pixels. It calculates the extent to which a pixel is correlated to its neighbors.

$$correlation = \sum_{i=0}^{K-1}\sum_{j=0}^{K-1} |i-j|.P(i,j) - \mu_x\mu_y/\sigma_x\sigma_y \quad (51)$$

where $p(i, j)$ is the intensity value of the pixel at the point (i, j). μ_x and μ_y means and SDs of the marginal distributions associated with $p(i, j)$.

4.2.11 | Homogeneity

It calculates how closely the elements of GLCM are distributed to the GLCM of nodule of interest.

$$Homogeneity = \frac{e^{-k(l(x,y)-l(i,j))^2}}{\sum_{i=1}^{m}\sum_{j=1}^{n} e^{-k(l(x,y)-l(i,j))^2}} \quad (52)$$

4.2.12 | Smoothness

The degree of asymmetry of a pixel distribution in the given image size $p \times q$ around the mean is expressed using the characteristics called as smoothness.

$$Smoothness = \sum_{1 \le k \le ng} \left(w_k \sum_{(p,q)\in N_k} \left| X_p^c - X_q^c \right| \right) \quad (53)$$

4.2.13 | IDM

It is used to measure of local homogeneity.

$$Inverse\ Difference\ Moment\ (IDM) = \sum_{i=0}^{k-1}\sum_{j=0}^{k-1} \frac{1}{1+(1-j)^2} P(i,j) \quad (54)$$

4.2.14 | RMS

It is used to see variation of image from its mean value.

$$RMS = \left[\frac{1}{N}\sum_{i=1}^{N} (w_i(x,y,t))^2\right]^{\frac{1}{2}} \quad (55)$$

For performance evaluation, the available FLIR dataset[37] of thermal imaging has been used. A total of 40 thermography images of the breast including 24 normal and 16 malignant is analyzed. Thirteen statistical

features were extracted based on GLCM, PCA and seven features were found to be statistically significant. Each statistical feature value was calculated as the average values obtained from four GLC matrices with one distance $d = 1$ pixel. The classifiers employed in this research are SVM, which is trained by a feature vector and tested. Using this technique, we used 30 images for training and remaining for testing.[31-32] This is then repeated for different enhancement techniques.

In Figure 6 explains the contrast comparison of input and proposed methods. These images clearly show the contrast of the proposed method is more efficient than previously used methods. The contrast of the proposed method in normal left is 0.2255 against the input image contrast of normal left 0.2175. Contrast of malignant right using adaptive method is 0.2205, Bi-histogram equalization is 0.2251 and CLAHE is 0.1892 against the contrast of input image 0.1725.

Figure 7 shows the correlation comparison of input and proposed method. In the first image, the correlation value of proposed method is 0.0908 against the correlation value of input image 0.09654. Second image, the correlation values using adaptive technology is 0.0975, Bi-histogram equalization is 0.0912 and CLAHE is 0.0989

FIGURE 7 Correlation comparison of input and proposed methods [Color figure can be viewed at wileyonlinelibrary.com]
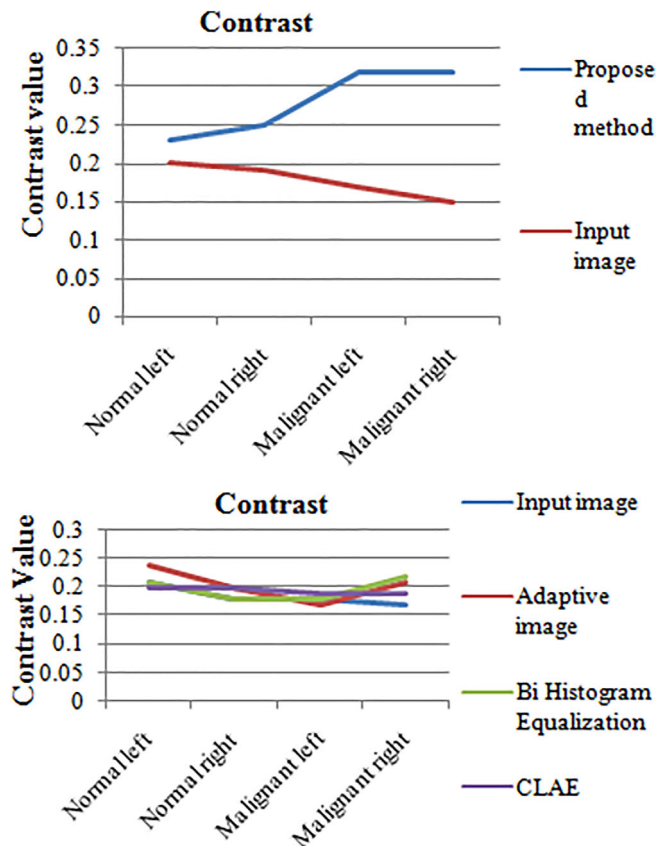
FIGURE 6 Contrast comparison of input and proposed methods [Color figure can be viewed at wileyonlinelibrary.com]
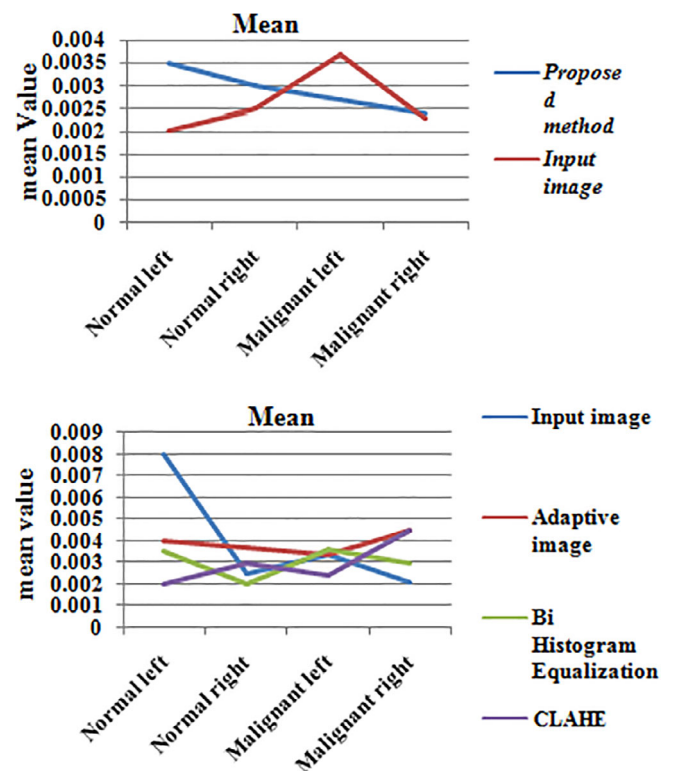
FIGURE 8 Mean comparison of input and proposed methods [Color figure can be viewed at wileyonlinelibrary.com]
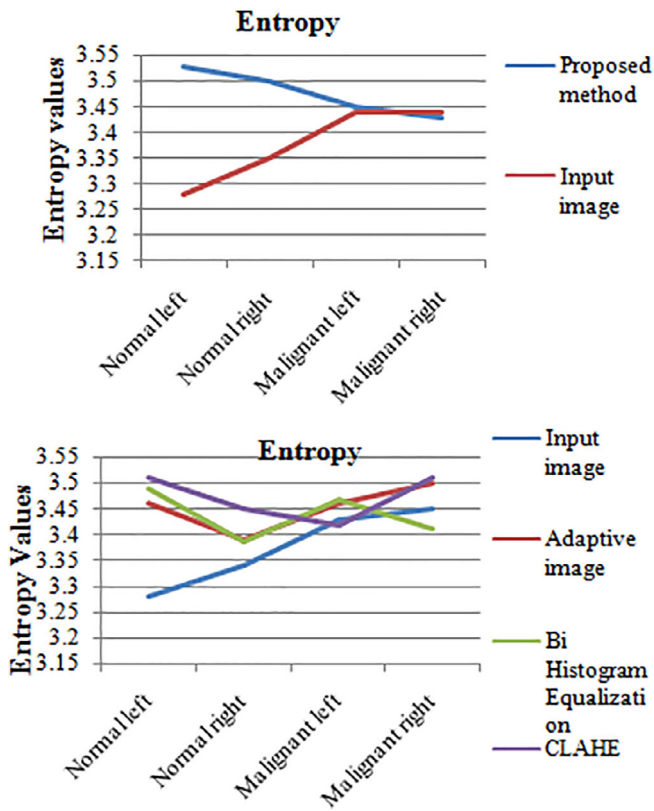
FIGURE 9 Entropy comparison of input and proposed methods [Color figure can be viewed at wileyonlinelibrary.com]
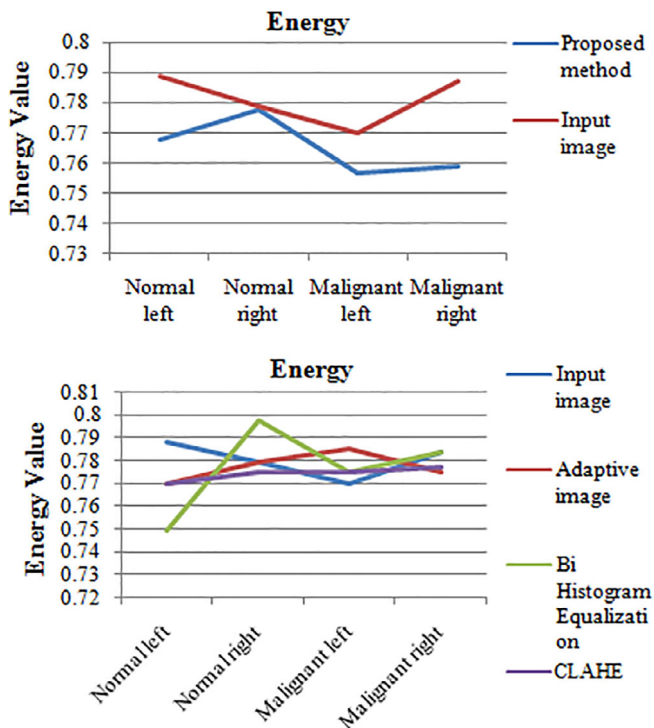
FIGURE 10 Energy comparison of input and proposed methods [Color figure can be viewed at wileyonlinelibrary.com]
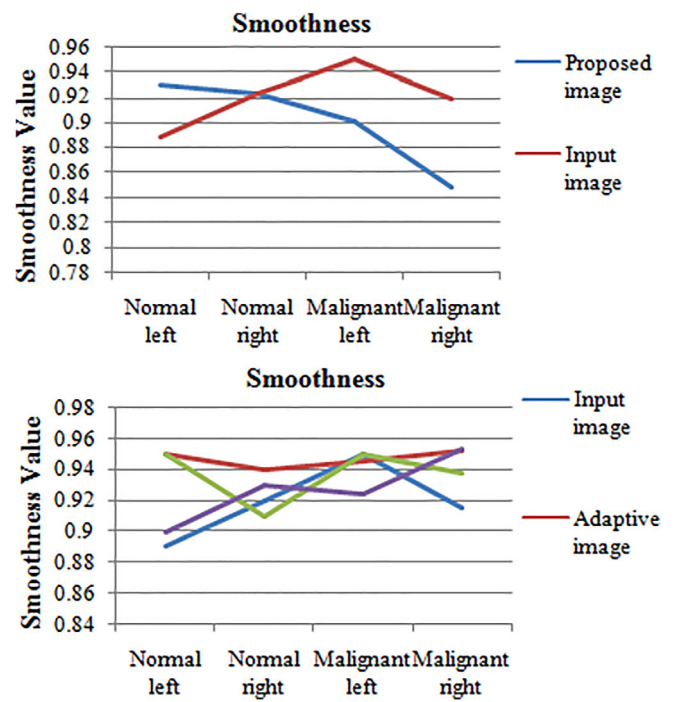
FIGURE 11 Smoothness comparison of input and proposed methods [Color figure can be viewed at wileyonlinelibrary.com]
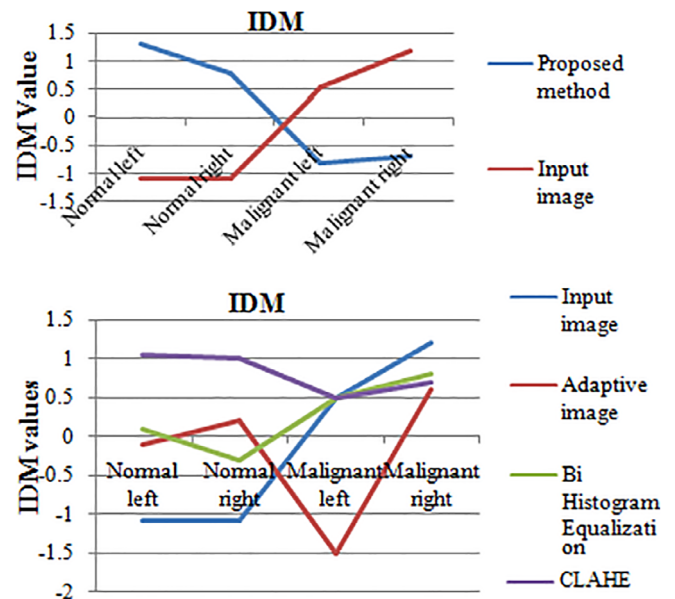
FIGURE 12 IDM comparison of input and proposed methods [Color figure can be viewed at wileyonlinelibrary.com]

against correlation of input image 0.1352. It clearly shows that correlation using the proposed method is better than the previously proposed methods.

In Figure 8 explains the mean comparison of input and proposed methods. Compare these two images it
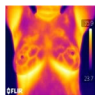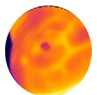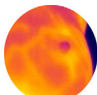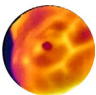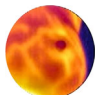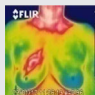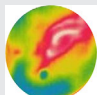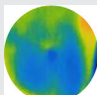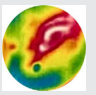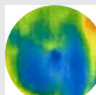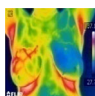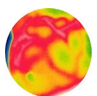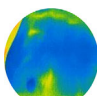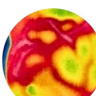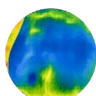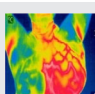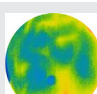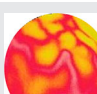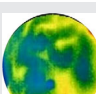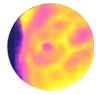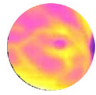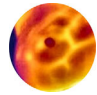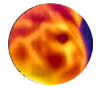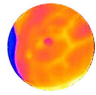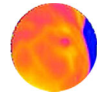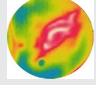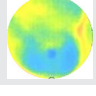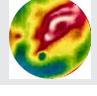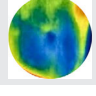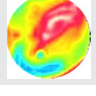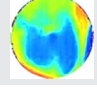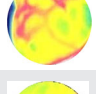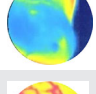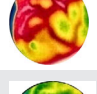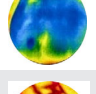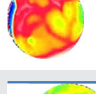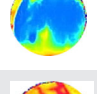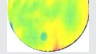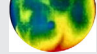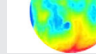
	Input image	Cropped input image		CLAHE	
		Right	Left	Right	Left
Normal 1					
Normal 2					
Malignant 1					
Malignant 2					

TABLE 2 Normal and malignant of input image, cropped ROI and CLAE enhanced [Colour figure can be viewed at wileyonlinelibrary.com]

TABLE 3 Enhancement of the normal and malignant image using Bi-histogram equalization, adaptive histogram and proposed method [Colour figure can be viewed at wileyonlinelibrary.com]

Input	Bi-histogram equalization		Adaptive histogram		Proposed	
	Right	Left	Right	Left	Right	Left
Normal 1						
Normal 2						
Malignant 1						
Malignant 2						

clearly shows that mean value using the proposed method 0.0023 against input image 0.0022. Second image shows the mean value of previously proposed methods. When we compare these two images the mean value using proposed method is accurate than the previously proposed methods.

In Figure 9, the entropy comparison of input and proposed method is shown. The entropy using the proposed method is 3.4373 against the input image 3.4514. The second image also shows the entropy value of different methods. From these two images we clearly understand the entropy value of different methods.

In Figure 10 shows the energy comparison of input and proposed methods. From the first figure the Energy value of input images is 0.7843 and proposed method is 0.7588. From the second image also shows the energy value of an image using different methods. From these two images we clearly understand the energy value of different methods.

In Figure 11 shows the smoothness comparison of input and proposed methods. From first image the smoothness of the input image is 0.9186 and proposed method is 0.8462. From the second image also shows the smoothness of the image in different methods. From these two images we clearly understand the smoothness value of different methods.

In Figure 12 shows the IDM comparison of input and proposed methods. From first image the IDM of input image is 1.2096 and proposed method is 0.2402. From the second image also shows the IDM of images in different

TABLE 4 Features extracted from normal image using various enhancement methods

	Input				Adaptive				Bi-histogram equalization				CLAHE				Proposed			
	NL	NR	ML	MR	NL	NR	ML	MR	NL	NR	ML	MR	NL	NR	ML	MR	NL	NR	ML	MR
Contrast	0.2112	0.2083	0.1931	0.1821	0.224	0.2098	0.1814	0.2115	0.2132	0.2097	0.1931	0.2164	0.2086	0.2093	0.1977	0.191	0.224	0.2406	0.3236	0.3223
Correlation	0.1145	0.1095	0.1121	0.0953	0.1105	0.1263	0.1175	0.0976	0.1217	0.1402	0.1121	0.0913	0.0751	0.1116	0.0862	0.1321	0.1163	0.1156	0.0984	0.0902
Energy	0.7881	0.778	0.7705	0.7843	0.7692	0.7786	0.7848	0.7756	0.7487	0.7977	0.7705	0.7834	0.7695	0.7745	0.7746	0.7771	0.7663	0.7768.	0.7554	0.7588
Homogeneity	0.9407	0.939	0.9383	0.9418	0.9357	0.9391	0.9421	0.9379	0.9310	0.9435	0.9383	0.94	0.9362	0.9392	0.9386	0.9383	0.9362	0.9362	0.9356	0.9327
Mean	0.008	0.0025	0.0037	0.0022	0.0041	0.0036	0.0034	0.0045	0.0037	0.0021	0.0037	0.003	0.0021	0.003	0.0024	0.0045	0.0035	0.003	0.0028	0.0023
SD	0.087	0.0857	0.0833	0.0833	0.087	0.0857	0.0833	0.0844	0.0870	0.0857	0.0833	0.0845	0.0884	0.0857	0.0833	0.0844	0.0884	0.0883	0.087	0.0883
Entropy	3.288	3.3421	3.436	3.4514	3.4624	3.3877	3.462	3.4994	3.4839	3.3849	3.436	3.4087	3.5089	3.4536	3.4221	3.5087	3.5363	3.5021	3.454	3.4375
RMS	0.087	0.0857	0.0833	0.0833	0.087	0.0857	0.0833	0.0845	0.0870	0.0857	0.0833	0.0845	0.0884	0.0857	0.0833	0.0845	0.0884	0.0884	0.087	0.884
Variance	0.0076	0.0073	0.0069	0.0069	0.0075	0.0073	0.0069	0.0071	0.0075	0.0073	0.0069	0.0071	0.0078	0.0073	0.0069	0.0071	0.0078	0.0078	0.0075	0.0078
Smoothness	0.8918	0.9235	0.9506	0.9186	0.9475	0.9424	0.9448	0.9552	0.9458	0.9059	0.9506	0.9371	0.9	0.9336	0.9238	0.9573	0.9285	0.9222	0.8909	0.8462
Kurtosis	7.782	7.4532	6.7663	6.0533	6.8922	7.2004	6.726	6.7203	5.9528	7.8794	6.7663	8.1369	6.2697	7.1923	6.7998	6.5543	7.6734	7.5918	7.0646	6.9626
Skewness	0.4253	0.3377	0.4518	0.3323	0.4386	0.5903	0.4232	0.4915	0.3778	0.5469	0.4518	0.5722	0.3009	0.4119	0.4278	0.5055	0.4966	0.6208	0.5863	0.4976
IDM	−1.0936	−1.0916	0.5084	1.2096	−0.0714	0.1883	−1.4636	0.5812	0.1918	−0.3536	0.5084	0.7936	1.0685	0.9667	0.4917	0.7185	1.2828	0.7407	−0.1903	−0.2402

TABLE 5 Features extracted from malignant image using various enhancement methods

	Input				Adaptive				Bi-histogram equalization				CLAHE				Proposed			
	NL	NR	ML	MR	NL	NR	ML	MR	NL	NR	ML	MR	NL	NR	ML	MR	NL	NR	ML	MR
Contrast	0.1901	0.1826	0.1846	0.1728	0.1907	0.2258	0.2143	0.2037	0.1812	0.1768	0.1746	0.1792	0.1971	0.1934	0.1996	0.2049	0.2276	0.2258	0.3226	0.3221
Correlation	0.1748	0.1163	0.0824	0.1585	0.1504	0.1093	0.1205	0.077	0.1409	0.1216	0.1258	0.1817	0.1238	0.1189	0.1135	0.0815	0.1883	0.1528	0.0953	0.0921
Energy	0.7761	0.7842	0.7844	0.7855	0.7837	0.7731	0.7843	0.7827	0.7621	0.7859	0.7659	0.7659	0.7901	0.7768	0.7848	0.7839	0.7635	0.7691	0.7592	0.7594
Homogeneity	0.9395	0.941	0.9408	0.941	0.9413	0.938	0.9412	0.9394	0.9366	0.9421	0.9372	0.9376	09426	0.9395	0.9413	0.9402	0.9324	0.936	0.9364	0.9408
Mean	0.0031	0.002	0.0003	0.0036	0.0029	0.0038	0.0034	0.0017	0.0029	0.003	0.0026	0.0038	0.0009	0.004	0.0025	0.0031	0.003	0.0037	0.0027	0.0021
SD	0.0842	0.0833	0.0833	0.0833	0.0845	0.0844	0.0845	0.0845	0.0833	0.0833	0.0833	0.0844	0.0845	0.0832	0.0833	0.0833	0.0833	0.0833	0.087	0.087
Entropy	3.4332	3.41	3.3063	3.5093	3.4337	3.4482	3.4678	3.4035	3.4321	3.511	3.4268	3.4907	3.3997	3.5029	3.3368	3.3871	3.5532	3.5503	3.485	3.4401
RMS	0.0845	0.0833	0.0833	0.0833	0.0845	0.0845	0.0845	0.0845	0.0833	0.0833	0.0833	0.0845	0.0845	0.0833	0.0833	0.0833	0.0884	0.0884	0.087	0.087
Variance	0.0071	0.0069	0.0069	0.0069	0.0071	0.0071	0.0071	0.0071	0.0069	0.0069	0.0069	0.0071	0.0071	0.0069	0.0069	0.0069	0.0078	0.0078	0.0075	0.0076
Smoothness	0.9385	0.9113	0.5958	0.9484	0.9317	0.9479	0.9406	0.8877	0.9360	0.9364	0.9311	0.9476	0.8231	0.9528	0.9264	0.9402	0.9229	0.9356	0.8195	0.8995
Kurtosis	7.1553	6.407	6.5349	6.5596	7.199	7.3725	7.1947	6.7292	5.7767	6.3309	5.8389	6.0935	7.8282	6.8345	7.5134	7.5584	6.8226	6.783	6.6311	7.5334
Skewness	0.547	0.3895	0.3732	0.3648	0.4682	0.6648	0.5848	0.5447	0.3234	0.2809	0.3225	0.4197	0.541	0.465	0.5581	0.5724	0.5493	0.5841	0.4661	0.6545
IDM	1.9081	−0.0231	−0.432	0.9981	0.2564	−0.3737	1.0393	−0.9487	−0.3704	−0.1638	−0.2547	0.9313	0.5478	0.4716	0.4979	0.3554	3.0672	0.4793	−1.5867	−0.4405

TABLE 6 SVM classifier output

Various enhancement method	Normal		Malignant		TP	TN	FP	FN
	Left	Right	Left	Right				
Input image	6	6	4	4	7	6	2	5
Adaptive histogram	2	2	2	2	9	7	1	3
Bi-histogram equalization	2	2	2	2	8	6	2	4
CLAHE	2	2	2	2	9	6	2	3
Proposed algorithm	6	6	4	4	11	7	1	1

Various enhancement method	Sensitivity (%)	Accuracy (%)	Specificity (%)
Adaptive histogram	75	80	87.5
Bi-histogram equalization	66.6	70	75
CLAHE	75	75	75
Proposed algorithm	91.6	90	87.5

TABLE 7 SVM classifier analyzing factors

methods. From these two images we clearly understand the IDM value of different methods.

In this paper, the enhancement techniques such as HE, CLAHE, AHE, BHE, and proposed approach are compared and it is depicted in Tables 2-5 and Figures 6-12. The existing color enhancement methods consequently change the quality of the image and our proposed power law transformation-based approach has an improved image quality with color enhancement for an easy and early detection of tumor. Tables 4 and 5, clearly depict the 13 statistical features were extracted using 4 levels of discrete wavelet transform (DWT) and have considerable variation between normal and malignant images. Based on the detailed performance evaluation of features of the proposed and the existing approaches were shown in Figures 6-12 and it is clearly evident that our proposed self-adaptive gray level histogram equalization technique achieves the best contrast enhancement for thermography images.

The results of the asymmetry analysis are compared and illustrated in Tables 6 and 7, it shows that, based on the given input images the normal and the malignant breast images identified as TP, TN, FP and FN values achieved through SVM classifier adapted with the various color enhancement approaches is tabulated. Similarly, by considering the metrics such as Sensitivity, Accuracy and Specificity of the thermography breast image by the SVM classifier adapted with the various color enhancement approaches are found to be 91.6%, 90%, and 87.5%. From the above comparative analysis, it is understood that the features were more accurately distinguishable after the enhancement by the proposed method, which improve the performance of the SVM classifier.

5 | CONCLUSION

In this work we have highlighted the necessity for the pre-processing techniques, the feature extraction techniques and color image enhancement techniques in IR image for an early detection of tumor. A Self Adaptive gray level Histogram equalization-based color enhancement algorithm is used in this work to improve the contrast of the input image which ensures the success of the consequent process. Then, the GLCM feature extraction technique is used to extract the features and a four-level DWT is applied to select the feature values that are different enough for several types, which helps the SVM based classifier system to identify the presence of cancerous tumor with high accuracy. The given input image for analysis is classified as normal or malignant by the classifier. The results displayed have validated the objective of this work. In future, we can extend the work based on multi-level classification by analyzing the degree of malignancy. Also, it classifies the given input as normal, benign and malignant, and improves the early detection of breast cancer.

CONFLICT OF INTEREST
Authors declare that they have no conflict of interest.

ORCID

Anthony Muthu Arul Edwin Raj 🔵 https://orcid.org/0000-0002-7788-4225

REFERENCES

1. Appukuttan A, S L. Breast cancer-early detection and classification techniques: a survey. *Int J Comput Appl.* 2015;132(11):9-13.

2. Malvezzi M, Carioli G, Bertuccio P, et al. European cancer mortality predictions for the year 2018 with focus on colorectal cancer. *Ann Oncol.* 2018;29(4):1016-1022.

3. Abdel-Nasser M, Moreno A, Puig D. Temporal mammogram image registration using optimized curvilinear coordinates. *Comput Methods Programs Biomed.* 2016;127:1-14.

4. Chiarelli A, Prummel M, Muradali D, et al. Digital versus screen-film mammography: impact of mammographic density and hormone therapy on breast cancer detection. *Breast Cancer Res Treat.* 2015;154(2):377-387.

5. Faust O, Rajendra Acharya U, Ng E, Hong T, Yu W. Application of infrared thermography in computer aided diagnosis. *Infra Phys Technol.* 2014;66:160-175.

6. Krawczyk B, Schaefer G. Breast thermogram analysis using classifier ensembles and image symmetry features. *IEEE Syst J.* 2014;8(3):921-928.

7. Mahmoudzadeh E, Montazeri M, Zekri M, Sadri S. Extended hidden Markov model for optimized segmentation of breast thermography images. *Infra Phys Technol.* 2015;72:19-28.

8. Diakides N. Infrared imaging: an emerging technology in medicine [from the guest editor]. *IEEE Eng Med Biol Mag.* 1998;17(4):17-18.

9. A breast cancer detection using image processing and machine learning techniques. *Int J Recent Technol Eng.* 2019;8(3):5250-5256.

10. Wang C, Ye Z. Brightness preserving histogram equalization with maximum entropy: a variation perspective. *IEEE Trans Consum Electron.* 2005;51(4):1326-1334.

11. Abdullah-Al-Wadud M, Kabir M, Akber Dewan M, Chae O. A dynamic histogram equalization for image contrast enhancement. *IEEE Trans Consum Electron.* 2007;53(2):593-600.

12. Ibrahim H, Pik Kong N. Brightness preserving dynamic histogram equalization for image contrast enhancement. *IEEE Trans Consum Electron.* 2007;53(4):1752-1758.

13. Sheet D, Garud H, Suveer A, Mahadevappa M, Chatterjee J. Brightness preserving dynamic fuzzy histogram equalization. *IEEE Trans Consum Electron.* 2010;56(4):2475-2480.

14. Wang C, Peng J, Ye Z. Flattest histogram specification with accurate brightness preservation. *IET Image Process.* 2008;2(5):249.

15. Nickfarjam A, Ebrahimpour-Komleh H. Multi-resolution gray-level image enhancement using particle swarm optimization. *Appl Intell.* 2017;47(4):1132-1143.

16. Rajinikanth V, Satapathy SC, Dey N, Vijayarajan R. DWT-PCA image fusion technique to improve segmentation accuracy in brain tumor analysis. *Microelectronics, electromagnetic and telecommunications.* Singapore: Springer; 2018:453-462.

17. Chu W, Ong C, Keerthi S. An improved conjugate gradient scheme to the solution of least squares SVM. *IEEE Trans Neural Netw.* 2005;16(2):498-501.

18. Acharya U, Ng E, Tan J, Sree S. Thermography based breast cancer detection using texture features and support vector machine. *J Med Syst.* 2010;36(3):1503-1510.

19. Marin ME, Vasilescu GM, Bârsan I, Kacso G, Rasnoveanu GV, Neacsu MG, Maricaru M, Demeter LN. Testing of two thermographic devices with two types of temperature sensors for detecting and locating of incipient breast tumors. 2018 International Symposium on Fundamentals of Electrical Engineering (ISFEE); 2018 (pp. 1–4). IEEE.

20. Roy A, Gogoi UR, Das DH, Bhowmik MK. Fractal feature based early breast abnormality prediction. In 2017 IEEE Region 10 Humanitarian Technology Conference (R10-HTC); 2017 (pp. 18–21). IEEE.

21. Singh D, Singh A. Role of image thermography in early breast cancer detection- Past, present and future. *Comput Methods Programs Biomed.* 2019;183:105074.

22. Dhal KG, Das A, Ray S, Gálvez J, Das S. Nature-inspired optimization algorithms and their application in multi-thresholding image segmentation. *Arch Comput Methods Eng.* 2020;27:855-888.

23. Transpire Online, (2019) Metaheuristic Anopheles Search Algorithm: An Natural Inspired Phenomena Utilized in Engineering Optimization Problems, Transpire Online; 2019. https://transpireonline.blog/2020/06/18/metaheuristic-anopheles-search-algorithm-an-natural-inspired-phenomena-utilized-in-engineering-optimization-problems/ Accessed October 2019.

24. Chakraborty J, Midya A, Mukhopadhyay S, et al. Computer-aided detection of mammographic masses using hybrid region growing controlled by multilevel thresholding. *J Med Biol Eng.* 2019;39(3):352-366.

25. Raghavendra U, Gudigar A, Rao T, Ciaccio E, Ng E, Rajendra Acharya U. Computer-aided diagnosis for the identification of breast cancer using thermogram images: a comprehensive review. *Infra Phys Technol.* 2019;102:103041.

26. Kim Y-T. Contrast enhancement using brightness preserving bi-histogram equalization. *IEEE Trans Consum Electron.* 1997;43(1):1-8.

27. Díaz-Cortés M, Ortega-Sánchez N, Hinojosa S, et al. A multilevel thresholding method for breast thermograms analysis using Dragonfly algorithm. *Infra Phys Technol.* 2018;93:346-361.

28. Gonzalez-Hernandez J, Recinella A, Kandlikar S, Dabydeen D, Medeiros L, Phatak P. Technology, application and potential of dynamic breast thermography for the detection of breast cancer. *Int J Heat Mass Transf.* 2019;131:558-573.

29. Tan S, Isa N. Exposure based multi-histogram equalization contrast enhancement for non-uniform illumination images. *IEEE Access.* 2019;7:70842-70861.

30. Madhavi V, Thomas CB. Multi-view breast thermogram analysis by fusing texture features. *Quant Infra Thermogr J.* 2019;16(1):111-128.

31. Devi RR, Anandhamala GS. Analysis of breast thermograms using asymmetry in infra-mammary curves. *J Med Syst.* 2019;43(6):146.

32. Abdel-Nasser M, Moreno A, Puig D. Breast cancer detection in thermal infrared images using representation learning and texture analysis methods. *Electronics.* 2019;8(1):100.

33. Jeyanathan JS, Shenbagavalli A, Venkatraman B, Menaka M, Anitha J, de Albuquerque VH. Analysis of transform-based

features on lateral view breast thermograms. *Circuit Syst Sig Process*. 2019;38(12):5734-5754.

34. Becker S. Foundations of Heat Transfer. Von FP Incropera, DP Dewitt, TL Bergman, AS Lavine. *Chem Ing Techn*. 2014;3(86): 395-396.

35. Usamentiaga R, Venegas P, Guerediaga J, Vega L, Molleda J, Bulnes F. Infrared thermography for temperature measurement and non-destructive testing. *Sensors*. 2014;14(7):12305-12348.

36. Das S, Gulati T, Mittal V. Histogram equalization techniques for contrast enhancement: a review. *Int J Comput Appl.* 2015; 114(10):32-36.

37. Pizer Stephen M, Amburn E. Philip, Austin John D., Cromartie R, Geselowitz A, Greer T, ter Haar Romeny B, Zimmerman J B, Zuiderveld K. Adaptive histogram equalization and its variations. *Comput Vis Graph Image Process*. 1987; 39(3):355-368.

38. Pisano E, Zong S, Hemminger B, et al. Contrast limited adaptive histogram equalization image processing to improve the detection of simulated spiculations in dense mammograms. *J Digit Imaging*. 1998;11(4):193-200.

39. Poddar S, Sharma D, Ghosh A, Tewary S, Karar V, Pal S. Non-parametric modified histogram equalization for contrast enhancement. *IET Image Process*. 2013;7(7):641-652.

40. Kandlikar SG, Perez-Raya I, Raghupathi PA, et al. Infrared imaging technology for breast cancer detection–Current status, protocols and new directions. *Int J Heat Mass Transf*. 2017;108: 2303-2320.

41. http://aathermography.com/breast/breasthtml/breasthtml.html.

42. Kallel F, Ben Hamida A. A new adaptive gamma correction based algorithm using DWT-SVD for non-contrast CT image enhancement. *IEEE Trans Nanobioscience*. 2017;16(8):666-675.